SHORT COMMUNICATION

Primary current distribution in the Hull cell and related trapezoidal geometries

A. C. WEST, M. MATLOSZ, D. LANDOLT

Ecole Polytechnique Fédérale de Lausanne, Laboratoire de Métallurgie Chimique, Département des Matériaux, MX-C Ecublens, CH-1015 Lausanne, Switzerland

Received 1 February 1991; revised 31 May 1991

Notation

a, b, A, B	parameters used to approximate the analytic solution, (see Equations 8, 9 and 10)
$i(x)/i_{avg}$	normalized current distribution
$(i(x)/i_{avg})_{app}$	approximation to the normalized current distribution
j	$\sqrt{(-1)}$
K_1, K_2, c, h'	constants used in the conformal mappings (see Equations 1 and 2 and Fig. 1)
$R\kappa\Delta$	dimensionless resistance of the cell shown in Fig. 1a
x, y	(dimensionless) real and imaginary components of the complex coordinate z
z, w, χ	coordinate systems used in the conformal mappings (see Fig. 1)
$\varepsilon(x)$	local error in the approximations to the current distributions, defined by Equation 11
θ	angle, radians (see Fig. 1a)
π	3.1415926 . . .

1. Introduction

An analytic solution of the primary current distribution of the cell shown in Fig. 1a is given. The geometry is important because it represents the Hull cell, frequently used in electroplating studies [1–3]. These geometries have also been used in levelling investigations as initial profiles in the simulation of shape changes [4]. Because the solution can be expressed simply (*i.e.*, a summation of an infinite series or a numerical integration is unnecessary), the formulae presented here can be useful for evaluating the accuracy of numerical procedures.

2. Analysis

A solution is obtained by a conformal mapping of the trapezoid of Fig. 1a into the rectangle of Fig. 1c. Moulton [5] was perhaps the first to use such techniques for the determination of a current distribution. Here, the conformal mapping is obtained in a straightforward manner by using two Schwartz–Christoffel transformations (see, for example, [6] or [7]). The three coordinate systems shown in Fig. 1 are related through

$$\frac{dz}{dw} = -jK_1 \frac{w^{\theta/\pi-1}(w-1)^{-\theta/\pi}}{(w-c-1)^{1/2}(w-c-2)^{1/2}} \quad (1)$$

and

$$\frac{d\chi}{dw} = -jK_2 \frac{w^{-1/2}(w-1)^{-1/2}}{(w-c-1)^{1/2}(w-c-2)^{1/2}} \quad (2)$$

The constants K_1 and c are determined by requiring that, when $w = 1$, $(x, y) = (1, \cot(\theta))$ and, when $w = 1 + c$, $(x, y) = (1, h + \cot(\theta))$. The details of the iterative numerical procedure, which requires repeated integrations of Equation 1 for assumed values of c, are similar to those described in references [8] and [9]. Once c is determined, K_2 is evaluated by requiring that, when $w = 1$, $(\chi_r, \chi_i) = (1, 0)$.

From Equations 1 and 2 and the Cauchy–Riemann equations, the potential gradients expressed in each of the coordinates shown in Fig. 1 can be related to one another. From these relationships, the local current density on the working electrode is found to be

$$\frac{i(x)}{i_{avg}} = \frac{K_2}{K_1 \sin\theta}\left(\frac{w}{1-w}\right)^{1/2-\theta/\pi} \quad (3)$$

where i_{avg} is the average current density. To use Equation 3, an explicit relationship between x and w is necessary (see Equation 1):

$$x = K_1 \sin\theta \int_0^w \frac{w^{\theta/\pi-1}(1-w)^{-\theta/\pi}dw}{(c+1-w)^{1/2}(c+2-w)^{1/2}} \quad (4)$$

With Equations 3 and 4, it can be seen that, for a given w (which varies between 0 and 1 on the working electrode) both the current density and the position on the electrode in 'real space' are obtained.

Large counterelectrode placements. The calculations described above show that, when $h > 2.5$, $c > 100$ for all θ. Consequently, the two terms in the denominator of the right side of Equation 1 are essentially constant when integrated from $w = 0$ to $w = 1$. An integration over this range of w gives

$$\lim_{c\to\infty} \frac{K_1}{c+1} = \frac{1}{\pi} \quad (5)$$

Equation 5 is obtained by relating Equation 1 to complete beta functions and gamma functions [10]. The final simplification is made with the reflectance formula [10].

It was also shown that the ratio $K_2/K_1 = 1.0$, and

0021-891X/92

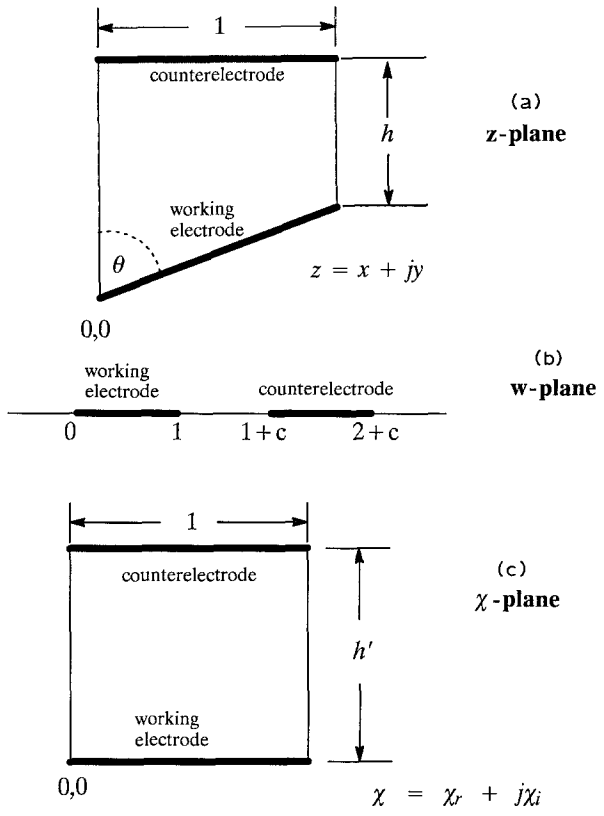

Fig. 1. (a) The electrochemical cell in Cartesian coordinates; (b) is an intermediate coordinate system used to obtain the mapping; (c) shows the geometry into which the trapezoid is mapped.

x is related to w through

$$x = \frac{\sin\theta}{\pi}\int_0^w w^{\theta/\pi-1}(1-w)^{-\theta/\pi}dw$$

$$= \frac{\sin\theta}{\pi}B_w(\theta/\pi, 1-\theta/\pi) \qquad (6)$$

where $B_w(\theta/\pi, 1-\theta/\pi)$ is the incomplete beta function [10]. The current distribution given by Equation 3 (with $K_2/K_1 = 1.0$) and Equation 6 are equivalent to the results first reported by Wagner* [11] for a counterelectrode placement at infinity. It is perhaps worth emphasizing that a counterelectrode placement at $h = 2.5$ gives nearly the same current distribution as a geometry with a counterelectrode placed at an infinite distance from the working electrode.

3. Curve fits to analytic solution

Many papers would be much more useful if numerical solutions or analytic solutions that require a numerical evaluation of an infinite series or an integral were fit to algebraic expressions. Unfortunately, curve fits seldom work satisfactorily unless the form of the fit has been suggested by solving a similar problem. Here, curve fits suggested from asymptotic analyses of the variation of the current distribution near the electrode edges are given. Their accuracies are also reported.

* Wagner chose not to utilize incomplete beta functions. Additionally the right side of his Equation 84 should be multiplied by cos (α), where α is defined in his paper.

For small distances from the electrode edges, asymptotic analyses of Equation 4 give analytic relationships between x and w. Combining these relationships with Equation 3 leads one to propose curve fits to the exact solution of the form

$$\left(\frac{i(x)}{i_{avg}}\right)_{app} = \left(\frac{x^a}{(1-x)^b}\right)(A + (B-A)x) \qquad (7)$$

where

$$a = (\pi/2\theta) - 1 \text{ and } b = (\pi - 2\theta)/2(\pi - \theta) \qquad (8)$$

The coefficients A and B can be predicted *a priori* from K_1, K_2, and c:

$$A = \frac{K_2}{K_1\sin\theta}\left(\frac{\theta(c+1)^{1/2}(c+2)^{1/2}}{K_1\pi\sin\theta}\right)^a$$

$$B = \frac{K_2}{K_1\sin\theta}\left(\frac{K_1\pi\sin\theta}{(\pi-\theta)c^{1/2}(c+1)^{1/2}}\right)^b \qquad (9)$$

3.1. *Hull cell*

For the Hull cell [1, 2, 3], $\theta = 0.22\pi$ radians and $h = 0.7385$ (after scaling). The numerical procedure discussed above gives $K_1 = 0.5112$, $K_2 = 0.4070$, and $c = 0.4803$. Equations 7, 8 and 9 give as an estimation of the current distribution:

$$\frac{i(x)}{i_{avg}} = \frac{x^{1.273}}{(1-x)^{0.359}}(1.733 - 0.763x) \qquad (10)$$

A comparison of Equation 10 with the current distribution obtained from Equations 3 and 4 shows that the maximum relative error in Equation 10 is 0.016 and occurs near $x = 0.35$. If greater accuracy is necessary, a fit of the error to a parabola can be used to give

$$\frac{i(x)}{i_{avg}} = \frac{x^{1.273}}{(1-x)^{0.359}}(1.733 - 0.763x)[1 + 0.065(x - x^2)]$$

$$|\varepsilon_{max}| \leqslant 0.003 \qquad (11)$$

Figure 2 compares the current distribution of the Hull cell predicted by Equation 10 to the numerical results of reference [3]. The solid line is the empirical equation given by norm DIN 50950 [12]:

$$\frac{i(x)}{i_{avg}} = 2.33\log(1/(1-x)) - 0.08 \qquad (12)$$

for $0.186 < x < 0.941$.

3.2. *Large counterelectrode placements*

For the case when $h > 2.5$, Equation (5) substituted into Equation 9 gives

$$A = \left(\frac{\theta}{\sin\theta}\right)^a\frac{1}{\sin\theta}$$

$$B = \left(\frac{\sin\theta}{\pi-\theta}\right)^b\frac{1}{\sin\theta} \qquad (13)$$

The local relative error $\varepsilon(x)$ in using Equations 7, 8 and 13, defined by

$$\frac{i(x)}{i_{avg}} = \left(\frac{i(x)}{i_{avg}}\right)_{app}(1 + \varepsilon(x)), \qquad (14)$$

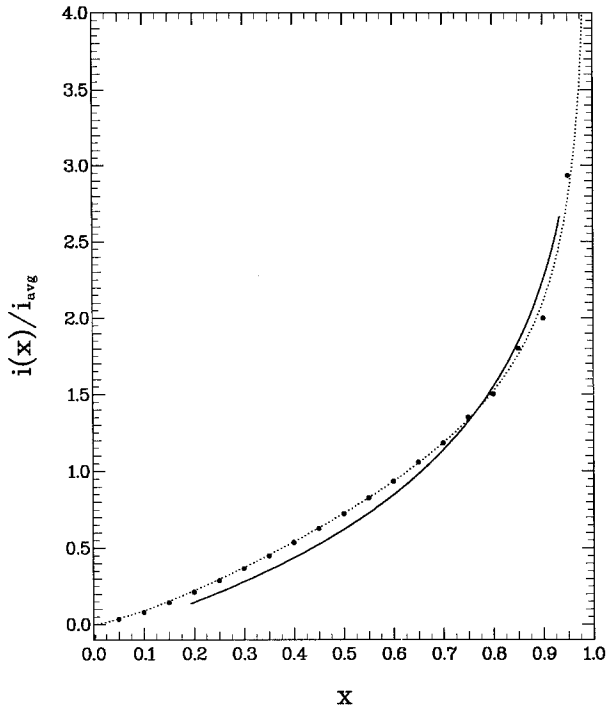

Fig. 2. The analytic solution for the primary current distribution of the Hull cell (dashed line) is compared to numerical results (points) previously reported in [3]. Also shown (the solid line) is an empirical formula given in [12].

was determined by comparisons with the exact solutions and is shown in Fig. 3. For $\theta \geqslant 0.2\pi$, the correction $\varepsilon(x)$ may not be important for many applications. In the event that the correction is important, Equations 3 and 6 can be used. (The incomplete beta function, B_w, is available in some commercial software packages [13]. Otherwise, it is tabulated [10] or can be evaluated numerically.)

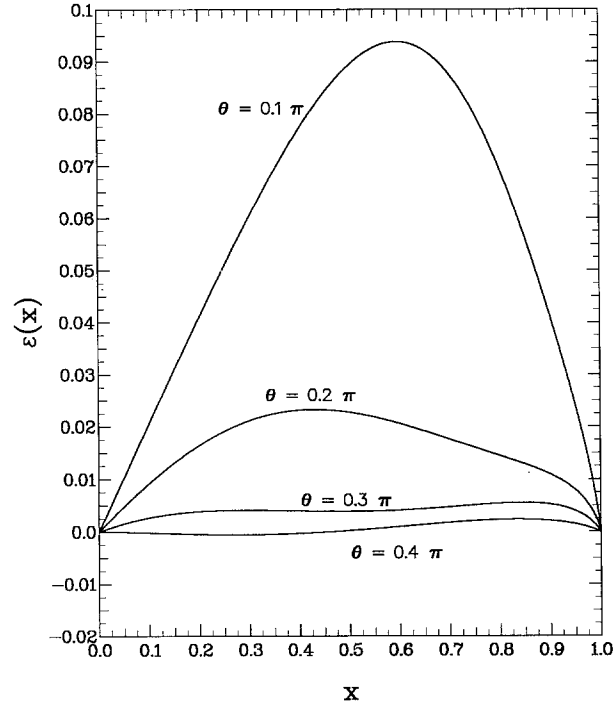

Fig. 3. The local error $\varepsilon(x)$ in the approximation of the current distribution by Equation 7 for the case when $h > 2.5$.

4. Ohmic resistance

By determining the average current density for a given potential difference between the working and counter electrodes, primary current distribution calculations also give the ohmic resistance of a cell. For the cell shown in Fig. 1a, the dimensionless ohmic resistance $R\kappa\Delta = h'$, where Δ is the width of the cell (perpendicular to the plane represented by Fig. 1a), κ is the electrolyte resistance, and h' is the dimensionless length shown in Fig. 1c, given by

$$h' = K_2 \int_1^{1+c} \frac{w^{-1/2}(w-1)^{-1/2}}{(c+1-w)^{1/2}(c+2-w)^{1/2}}\,dw \tag{15}$$

For the Hull cell, $h' = 1.041$. The numerical results for the Hull cell (shown in Fig. 2) were obtained without accounting explicitly for the singularities at the electrode edges. Consequently, at $x = 1$, the numerical solution predicts a finite current density, which gives an average current density that it is too low. This, in turn, gives an ohmic resistance that is approximately five percent too high. (We did not pursue in detail how this error varies, for example, with mesh spacing).) Contrary to what might be expected, the boundary element method gives for this case an accurate current distribution, but a relatively inaccurate ohmic resistance. These observations indicate the importance of assessing quantitatively the error in numerical calculations, even though, for practical problems, this can be very difficult.

Acknowledgements

Financial support for this project was provided by the Office Fédéral de l'Éducation et de la Science, Bern, Switzerland.

References

[1] R. O. Hull, *Am. Electroplat. Soc.* **27** (1939) 52.
[2] W. Nohse, 'Die Untersuchung galvanischer Bäder in der Hull-Zelle', 3rd edition, Verlag Saulgau, Germany (1984).
[3] M. Matlosz, C. Creton, C. Clerc, and D. Landolt, *J. Electrochem Soc.*, **134** (1987) 3015.
[4] C. Clerc and D. Landolt, *Electrochim. Acta* **29** (1984) 787.
[5] H. Fletcher Moulton, *Proc. London Math. Soc.* (*ser.* 2) **3** (1905) 104.
[6] L. A. Rubenfeld, 'A First Course in Applied Complex Variables,' McGraw-Hill, New York (1985).
[7] R. V. Churchill, 'Complex Variables and Applications,' 2nd edition, McGraw-Hill, New York (1960).
[8] M. E. Orazem and J. Newman, *J. Electrochem Soc.* **131** (1984) 2857.
[9] Conrad B. Diem, Bernard Newman, and Mark E. Orazem, *J. Electrochem Soc.* **135** (1988) 2524.
[10] M. Abramowitz and I. Stegun, 'Handbook of Mathematical Functions,' National Bureau of Standards, Washington (1964) chap. 6.
[11] C. Wagner, *J. Electrochem. Soc.* **98** (1951) 116.
[12] Norm 50950 DIN (Deutsches Institut für Normung), Mikroskopische Messung der Schichtdicke, TAB 175, Beuth Verlag GmbH, Berlin Köln (1983).
[13] S. Wolfram, 'Mathematica. A system for Doing Mathematics by Computer,' Addison-Wesley, New York (1988).